Received: 28 May 2018 | Revised: 12 June 2018 | Accepted: 29 June 2018

DOI: 10.1111/eci.12992

REVIEW

WILEY

Role of hemodynamics in initiation/growth of intracranial aneurysms

Mannekomba R. Diagbouga[1] | **Sandrine Morel**[1,2] | **Philippe Bijlenga**[2] | **Brenda R. Kwak**[1]

[1]Department of Pathology and Immunology, Faculty of Medicine, University of Geneva, Geneva, Switzerland

[2]Neurosurgery Division, Department of Clinical Neurosciences, Faculty of Medicine, Geneva University Hospitals, Geneva, Switzerland

Correspondence: Brenda R. Kwak, PhD, Department of Pathology and Immunology, University of Geneva, CMU - lab F06.2764.a, Rue Michel-Servet 1, CH-1211 Geneva 4, Switzerland (Brenda.KwakChanson@unige.ch).

Funding information
Swiss Heart Foundation; Swiss SystemsX.ch, Grant/Award Number: MRD-AneuX-2014/261

Abstract

Background: Intracranial aneurysm (IA) is a disease of the vascular wall resulting in abnormal enlargement of the vessel lumen. It is a common pathology with a prevalence of 2%-3% in the adult population. IAs are mostly small, quiescent and asymptomatic; yet, upon rupture, severe brain damage or even death is frequently encountered. In addition to clinical factors, hemodynamic forces, mainly wall shear stress (WSS), have been associated with the initiation of IAs and possibly with their risk of rupture. However, the mechanism by which WSS contributes to aneurysm growth and rupture is not completely understood.

Design: PubMed and Ovid MEDLINE databases were searched. In addition, key review articles were screened for relevant original publications.

Results: Current knowledge about the relation between WSS and IA has been obtained from both computational fluid dynamic studies in patients and experimental models of IA formation and growth. It is increasingly recognized that a high wall shear stress (gradient) participates to IA formation and that both low and high WSS can drive IA growth. Primary cilia (PC) play an important role as mechanosensors as patients with polycystic kidney disease, which is characterized by the absence or dysfunction of PC, have increased risk to develop IAs as well as increased risk of rupture.

Conclusion: Wall shear stress is a key player in IA initiation and progression. It is involved in vascular wall remodelling and inflammation, processes underlying aneurysm pathophysiology.

KEYWORDS
endothelium, intracranial aneurysms, primary cilium, wall shear stress

1 | INTRODUCTION

Intracranial aneurysm (IA) is a disease of brain arteries, which results in 90% of cases in a balloon-like enlargement of the vessel lumen, whereas the other 10% account for fusiform, dissecting and mycotic aneurysms.[1] When the aneurysm ruptures, it causes bleeding in the subarachnoid space leading to severe disabilities or even death of the patient. Despite the fact that most IAs are asymptomatic, there is a growing number of IA detected as a result of increasing screening with modern imaging modalities. The prevalence of IA in the adult population is between 2% and 3%[2] and the risk of rupture has been estimated between 0.3% and 15% per 5 years.[3] There is no medical treatment to prevent the unruptured IA from rupturing, and currently, this can be performed only with endovascular or open microsurgical occlusion of the aneurysm. However, surgical clipping or endovascular coiling is associated with 6.7%[4] and 4.8%[5] unfavourable outcomes, respectively. Given the high risk of complications, it is essential to identify IAs

prone to rupture and to evaluate the balance between risk and benefit of treatment. Individual patient's characteristics, such as gender, age, familial history, hypertension and autosomal dominant polycystic kidney disease (ADPKD) as well as aneurysm dome characteristics, such as size, location, and shape irregularities, may be conjointly used for this purpose. Indeed, prediction tools for IA growth and/or rupture such as PHASES,[6] UIATS[7] and ELAPSS[8] scores have been developed based on these risk factors to help for decision-making onto treatment of unruptured IAs. Even if these tests are easily applicable and correlate well with the severity of the disease, they have numerous limitations and thus need more validation.[6-9] For instance, aneurysm size remains a major criterion for treatment as it is assumed that large IAs are at higher risk for rupture than small IAs. However, small IAs with regular shape may also rupture.[10] Therefore, it has been suggested that growing aneurysms independently of their size are more likely to rupture.[11,12] Hence, more factors signifying the biological processes leading to growth and rupture should be considered for decisions onto treatment of unruptured IAs. Indeed, there is increasing evidence showing that hemodynamic forces exerted on the vessel wall by the flowing blood may induce vascular remodelling leading to IA formation, growth and rupture.[10,13-20] Hemodynamic forces may thus be considered as additional prediction factors for IA outcome.[19,21] In this review, we will focus on the influence of hemodynamic forces on IA pathogenesis as well as on mechanoreceptors and intracellular signalling pathways that mediate vascular wall remodelling.

2 | BIOMECHANICAL FORCES ACTING ON THE ARTERIAL WALL

The viscous and pulsatile nature of blood flow exposes arteries to different mechanical forces, such as the wall shear stress (WSS). The WSS represents the drag force per unit area imposed by the flowing blood on the vessel wall, parallel to the flow direction. In the healthy human aorta, WSS forces range between 10 and 20 dynes/cm^2 (1 Pa = 1 N/m^2 = 10 dynes/cm^2)[22] and this value slightly increases in arteries with smaller diameters like cerebral arteries.[23] The WSS can be calculated using the Hagen-Poiseuille formula: $\tau = 4\mu Q/\pi r^3$, where τ is the shear stress, μ is the blood viscosity, Q is the volumetric flow rate, and r is the lumen radius.[24] Using this formula implies that the vessel is a straight, uniform and stiff tube; and that blood is an incompressible Newtonian fluid (constant viscosity) and that flow is constant and laminar. These compromises are acceptable for WSS measurement in large and straight arteries where blood flow approximates Newtonian fluid behaviour.[24] However, in reality, blood flow is unsteady and indeed a non-Newtonian fluid. Moreover, the arterial system is a network of branched and curved vessels where blood flow patterns become complex due to flow separation and reversal, and to spatial and temporal variations. Thus, WSS calculation should include additional parameters among which the Reynolds number (Re) describing the ratio between inertial and viscous forces and representing the stability of the flow; the Womersley number (α) that is the expression of the pulsatile flow frequency in relation to viscous effects; the Dean number (Dn) depicting the effect of curvature of a vessel on the flow profile.[25] The WSS complex calculation in the circle of Willis can thus be achieved using computational fluid dynamics (CFD).[26,27] The pulse pressure variation of the blood flow induces the stretching of the vascular wall. Indeed, during the systole, the aorta undergoes approximately 10% circumferential stretch and this value decreases to approximately 5% in peripheral arteries.[28] This mechanical distension of the vessel is referred as cyclic circumferential stretch (CCS). Endothelial cells (ECs) sense finely the WSS while effects of CCS are typically studied in both ECs and smooth muscle cells (SMCs).[28] Under normal range of flow/pressure, vascular cells respond through mechanoreceptors by triggering and releasing biochemical signals, which maintain the physiological function of blood vessels. Pathological conditions, instead, would trigger degenerative remodelling leading to an instable artery wall. This wall instability may favour aneurysm initiation, growth and rupture. While the WSS is known to have a critical role in IA disease, the influence of CCS still needs to be clarified and will not be discussed in this review.

3 | LOCALIZATION OF IAS

Intracranial aneurysms appear mainly at or near bifurcations in the circle of Willis, which is a circle of communicating brain arteries. Blood is supplied to the brain principally through two internal carotid arteries and two vertebral arteries. The internal carotid arteries irrigate principally the cerebrum whereas the vertebral arteries join to form the basilar artery that irrigates the rest of the brain and part of the cerebrum. The internal carotid arteries and the basilar artery are connected through the circle of Willis. In humans, this circle is formed mainly by the anterior cerebral arteries, anterior and posterior communicating arteries and posterior cerebral arteries (Figure 1). The ring-like structure of the circle of Willis provides a collateral circulation of blood, allowing the irrigation of the brain in case of artery occlusion or absence. However, this peculiar arterial network is exposed to a unique hemodynamic pattern comprising impinging, converging, dividing, swirling and secondary flow.[29,30] Hence, anatomical variation in the

circle of Willis such as hypoplasia or absence of an arterial segment would affect hemodynamic parameters, which may lead to cerebrovascular disease. Indeed, abnormal circle of Willis has been associated with high risk of IA development[31] and rupture,[32] which may be the resultant of abnormal WSS.[33,34] As approximately 40% of the population has an incomplete circle of Willis, it suggests that even if hemodynamic factors are key players in IA development, other additive factors might be required.[32,35]

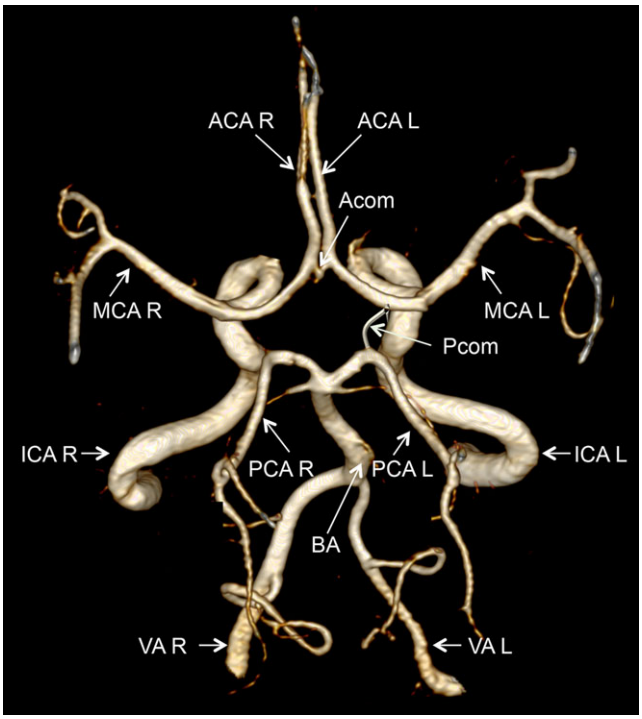

FIGURE 1 Angiographic image of a human circle of Willis. Indicated are vertebral arteries (VA), right (R) and left (L), basilar artery (BA), internal carotid arteries (ICA R, ICA L), posterior cerebral arteries (PCA R, PCA L), anterior cerebral arteries (ACA R, ACA L), middle cerebral arteries (MCA R, MCA L), posterior communicating artery (Pcom) and anterior communicating artery (Acom)

4 | PATHOGENESIS OF IAS

The wall of large arteries is composed of three main layers: the *tunica intima* that is the innermost layer consisting of the endothelium and the supportive basement membrane; this is followed towards the exterior side by a SMC layer with elastin and collagen fibers forming together the *tunica media*; the last layer is the *tunica adventitia,* which is the outer connective tissue (mostly composed of collagen fibers and fibroblasts). Depending on the artery size, the *tunica media* is outlined either by an internal elastic lamina (IEL) separating the media from the intima, and/or an external elastic lamina (EEL) separating the media from the adventitia. The role of the elastic lamina is to accommodate blood volume fluctuations. Cerebral arteries have a well-developed IEL but lack the EEL (Figure 2A). Moreover, the low amount of connective tissue within subarachnoid space together with the thin media and adventitia of cerebral arteries make them more susceptible to hemodynamic forces and at risk to develop aneurysms.[36] Histologically, the aneurysmal wall composition and organization are quite different from the ones of a healthy cerebral artery (Figure 2A-D). The first histological alteration of cerebral arteries leading to IA formation is the destruction of the IEL.[27,37,38] Although the histological evolution between a healthy cerebral artery to the different steps of IA growth and rupture is not completely known, several studies have shown that the lack of IEL is associated with erosion of luminal endothelium, infiltration of inflammatory cells, loss of SMCs, destruction of the extracellular matrix (ECM),

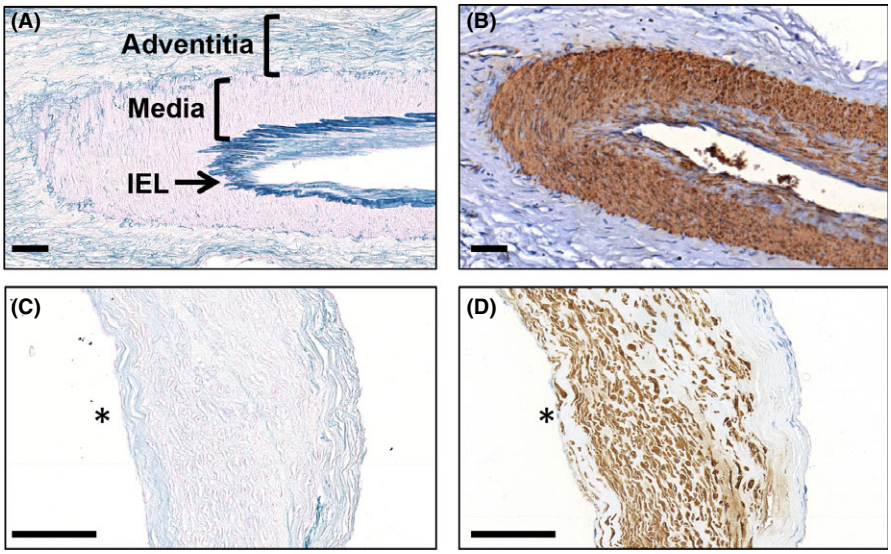

FIGURE 2 Histological images of a human temporal artery (A and B) and human intracranial aneurysm (IA; C and D). Paraffin sections were stained for Victoria blue (A and C, elastin in blue) or alpha smooth muscle actin (B and D, smooth muscle cells [SMCs] in brown). For experimental details, we refer to Morel et al.[44] The healthy artery has a well-defined internal elastic lamina (IEL) and media with organized SMCs. The IEL is absent in the IA dome and the medial layer shows disorganized SMCs. Scale bars = 100 μm. Asterisk indicates the arterial lumen

activation of the innate immunity, calcification and/or lipid accumulation.[39-44] Frösen et al[39] have classified the IA wall in 4 groups using the following parameters: (a) endothelialized wall with linearly organized SMCs; (b) thickened wall with disorganized SMCs; (c) hypocellular wall with either intimal hyperplasia or organizing luminal thrombosis; (d) an extremely thin thrombosis-lined hypocellular wall. Based on this classification, it has been shown in Finnish[39] and Swiss[44] cohorts of patients affected by IA that ruptured aneurysmal domes are in vast majority histologically characterized by hypocellular and/or very thin vascular walls and luminal thrombosis (grades c and d). In contrast, unruptured IAs contain ECs and/or a thickened media with SMCs (grades a and b). From these studies, one may hypothesize that loss of SMCs would make the IA wall susceptible for rupture. In consequence, aneurysmal SMC content may then serve as a marker for IA stability.

5 | WSS AND IA DEVELOPMENT

5.1 | The role of WSS on vascular function

Unidirectional laminar high WSS (HWSS) experienced by ECs in straight part of the arterial tree is assigned as physiological flow as it promotes a quiescent and cytoprotective state: ECs are aligned in the direction of the flow, and anti-inflammatory and antithrombotic gene expression is induced by the transcription factors KLF2, KLF4 and Nrf2.[22] Altered blood flow inducing sustained supraphysiological (high) WSS (SWSS) or low WSS (LWSS) may induce EC dysfunction and damage of the vascular wall through different mechanisms.[45] Oscillatory wall shear stress (OWSS) representing reversal of the blood flow direction can exacerbate the endothelium dysfunction.

Low WSS-mediated EC dysfunction is associated with an altered morphology of ECs (cobblestone instead of elongated shape), a high turnover, increased permeability and migration.[22,46] LWSS is also known to generate oxidative stress, through enhanced superoxide production, resulting in impaired eNOS/COX-2 activity and consequently reduced NO/PGI_2 bioavailability.[22,46,47] This is followed by an increased expression of vascular cell adhesion and chemotactic molecules on the surface of ECs, promoting thereby an inflammatory and pro-thrombotic environment.[47,48] Moreover, inflammatory cell recruitment and transmigration through the endothelium can drive vessel wall degeneration by metalloproteinase (MMP) production and activity.[49]

Supraphysiological wall shear stress regions have been shown to correlate with reduced eNOS expression in ECs and the induction of iNOS in SMCs. The excessive NO production by iNOS can increase peroxynitrite synthesis leading to cell apoptosis and MMP activation.[50] Moreover, an increased MMP2 and MMP9 expression was observed in areas of SWSS compared to physiological HWSS regions, conjointly with reduced proliferation rate and loss of SMCs.[50] The loss of ECs may be explained by the disappearance of eNOS, which has been linked to loss of intercellular contacts. In addition, apoptotic, reorienting and dividing ECs can also be lost by mechanical detachment. Dolan et al[51] showed that, in vitro, SWSS leads to impaired alignment and high turnover of ECs. Furthermore, transcriptional profiles of ECs exposed to SWSS confirmed the active remodelling process through matrix degradation and re-synthesis. An exacerbation of this phenotype is observed when SWSS is combined with a steep increasing WSS gradient (WSSG).

5.2 | IA initiation

Analysis of cerebral arteries from autopsy and IA animal models allowed characterizing the early changes in the nascent aneurysm. The aneurysm wall is commonly described having a disrupted IEL, a media thinning and a bulge formation.[27,38,52] The aetiology of IAs has been subject of debate for a long time, with postulation of different theories. The first theory proposed a congenital cause, whereas the second theory assumed that IAs are acquired lesions during lifetime with hemodynamic factors playing an important role.[38] Indeed, the preferential location of the aneurysm at arterial bifurcations exhibiting a specific flow pattern suggested an implication of hemodynamics in the initiation of aneurysm formation. Meng et al[27] sought to understand how "an hemodynamic insult" could lead to a maladaptive remodelling of the vessel wall. Using CFD, they discriminated three regions at arterial bifurcations with different blood flow patterns: the impingement zone, where blood from the parent artery hits the apex of the bifurcation and creates a stagnation point before accelerating into the branches (WSS $\leq$ 20 dynes/cm^2; velocity $<$ 0.05 m/s; positive WSSG); the acceleration region, where blood flow continues to accelerate until the maximum velocity (WSS $>$ 20 dynes/cm^2, high positive WSSG); and the recovery region where the velocity of blood reaches the maximum and starts to decelerate until the physiological level of WSS ~20 dynes/cm^2 (negative WSSG). By mapping CFD with histological analysis of the arterial bifurcation, they reported early changes resembling IA initiation in regions submitted to SWSS and positive WSSG.[27] These findings were supported by further studies indicating that aneurysmal remodelling occurs only when hemodynamic forces go beyond a certain threshold (WSS $>$ 1.22×10^3 dynes/cm^2 and WSSG $>$ 530 Pa/mm) in their rabbit model.[52] Although these results help to understand the role of hemodynamic forces in IA initiation, the study of Meng et al was performed on an artificial extracranial

bifurcation in a low number of animals and needs further confirmation in other preferably intracranial animal models. Furthermore, the provided hemodynamic threshold values only stand for rabbit and may differ in human where the vessel diameter is different and numerous confounding factors would affect IA development, such as inherited risk factors and habits. However, the concept of WSS threshold could explain why IAs develop more frequently at certain bifurcations and individuals than others. Each arterial bifurcation has a specific flow pattern owed to the location, the bifurcation angle, and the parent and daughters vessel size making some more prone to reach the threshold. For example, an already weakened wall caused by ageing, smoking, hypertension and inherited diseases would have a lower tolerance to hemodynamic disturbances. Meta-analysis in patients correlating hemodynamic forces and IA development support the fact that IAs are triggered by SWSS and positive WSSG.[53,54]

5.3 | IA growth and rupture

The exact mechanisms leading to IA growth and rupture are not yet well understood. It is assumed that IA growth results from a combination of vessel wall remodelling and wall distension, whereas rupture occurs when the wall is too weak to resist to the tension induced by the blood pressure.[55]

There are conflicting results concerning the impact of high or low WSS in aneurysm growth and rupture. CFD analysis comparing ruptured and unruptured IAs showed in some studies that LWSS promotes IA growth and rupture,[13,16-19,54] while others have shown that SWSS was related to these events.[14,15,56,57] The discrepancy of results regarding WSS demonstrates the challenge of understanding IA pathology. Unfortunately, studies are usually performed on limited sample numbers and the diversified experimental design (eg, imaging tool, CFD boundaries conditions) further enhances the inconsistency in the results. It is also important to note that the correlation of WSS with IA risk of rupture is generally performed on ruptured vs unruptured aneurysms.[14,15] Knowing that the shape of the aneurysm can change after the rupture, it could impact on blood flow dynamics and resulting forces. In addition, even though CFD analysis has gained power over the years, there is still a need to improve the precision of the method and to have more unified boundaries conditions. However, the complexity and heterogeneity seen in IA progression could also reflect the existence of several mechanisms.[45] Co-existence of the LWSS and the SWSS theories has been proposed.[55,58] For example, small IAs with a thin, smooth, hypocellular and translucent wall would result from SWSS-driven degradation mechanisms, whereas thick-walled large IAs with irregular surface would result from LWSS-driven inflammatory pathways. Intermediate IA phenotypes would result from an interplay between low and high WSS pathways.[55] In support of this hypothesis, a relationship between WSS profile and IA phenotype was demonstrated.[58] To better clarify the role of WSS in aneurysmal disease, we need to first understand the interaction of the vessels with hemodynamic forces and the biological processes mediating IA growth and rupture.

6 | ECS AND SHEAR STRESS MECHANOTRANSDUCTION

The biological and phenotypic adaptation of ECs according to the flow is likely due to their ability to sense the microenvironment. The mechanism by which ECs sense external forces applied to their surface and convert it into intracellular biochemical responses is called mechanotransduction. ECs respond to changes in WSS in a timeframe ranging from seconds up to several minutes. The responses involve numerous mechanosensors and signalling molecules.[22]

6.1 | Mechanosensors of wall shear stress

The force transmission to the cell is mediated by several cellular components (Figure 3). The plasma membrane itself has been shown to be WSS sensitive. Remodelling of the phospholipid bilayer can occur few seconds after onset of shear stress with potential alteration of the protein organization and activity resulting in downstream activation of signalling pathways.[59] Several ion channels including K^+, Na^+, Ca^{2+}, TRPV (transient receptor potential cation channel) and Piezo 1/2 channels mediate the endothelial response to WSS. For instance, expressing K^+ channels into *Xenopus laevis* oocytes turns them sensitive to shear stress.[60] The glycocalyx, a polycarbonate coat that covers the cell membrane, is also regulated by the WSS. It has been shown that knocking-down some core proteins of the glycocalyx leads to a failing of WSS-induced eNOS and cytoskeleton remodelling.[60] Caveolae are cholesterol- and sphingolipid-rich microdomains that contain high levels of caveolin and cavin family proteins. Caveolae are cup-like invaginations containing many receptors and signalling molecules that may function as a signalling platform. The flattening of these structures by WSS or stretch would activate caveolin and induce responses through ERK, Rho GTPases, eNOS, Src family kinase and Akt activation.[60] Primary cilia (PC) are microtubule-based organelles that protrude at the apical side of most differentiated cells (ie, kidney, retina, liver epithelial cells, neuronal and vascular cells) and have numerous functions (chemosensing, mechanosensing, olfaction, photoreception). Their role in WSS sensing and in aneurysm development has been well

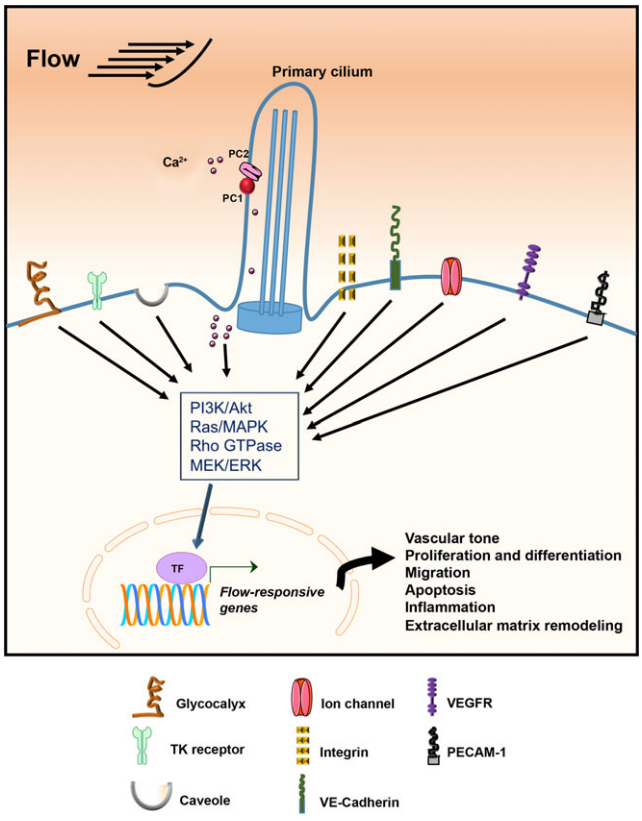

FIGURE 3 Schematic representation of wall shear stress mechanosensors at the endothelial surface. The activation of mechanosensors by shear stress triggers a cascade of signalling pathways modulating gene expression and endothelial cell function

established in several studies[61-63] (see section 6.3). Integrins, the proteins connecting the cell to the ECM, can also mediate WSS-induced responses. WSS induces activation of integrins, which undergo conformational changes and modulate their affinity for cytoskeleton or ECM proteins. Adherens junction proteins, principally VE-cadherin, can also transmit extracellular force. In association with PECAM-1 and VEGFR2/3, VE-cadherin forms a mechanoresponsive complex, which stimulation leads to activation of the pro-inflammatory NF-κB pathway.[60] A central core of WSS responsive elements is the cytoskeleton, whose remodelling is part of the early changes induced by flow. Indeed, the cytoskeleton binds to most of the sensors cited above and therefore ties them together. This configuration helps the transmission of a force applied locally at one site of the membrane to a distant site allowing for an efficient and complete adaptive response to stress.[60] Finally, another fundamental player in mechanotransduction is the nucleus. Disruption of nucleus envelope proteins leads to impaired mechanotransduction signalling. Even if the nucleus is not a direct sensor of WSS, it establishes the link between force transmission and biochemical signalling.[64]

6.2 | Mechanosensing and intracellular signalling

The activation of mechanosensors by WSS triggers a cascade of signalling pathways and modulates genes expression. Physiological unidirectional laminar HWSS regulates genes involved in vascular endothelial homoeostasis keeping the endothelium in a quiescent, anti-inflammatory and antithrombotic state. For example, under physiological HWSS, eNOS expression is regulated by a delicate balance between Akt phosphorylation-mediated activation[65] and PYK2-mediated repression.[66] KLF2, which positively regulates eNOS, has a sustained expression, involving the ERK5-MEF2 signalling cascade[67] and miR-92a repression, which is a negative regulator of KLF2.[68] In addition, physiological HWSS has a negative regulation of Ras GTPase/MAPK kinases signalling, thus, repressing inflammatory gene expression. Indeed, NO production inhibits PKC-ε and ERK1/2 leading to the repression of MCP-1.[69] In addition, AMPK/PARP-1/Bcl6 signalling inhibits VCAM-1, MCP-1 and MCP-3 expression.[70] Finally, physiological HWSS sustains quiescence of ECs by activating genes that promote growth arrest (GADD45, p21) and abrogate apoptosis via activation of signalling pathways involving superoxide dismutase and NO synthase.[22]

In contrast, disturbed flow promotes pro-inflammatory gene and adhesion protein expression as well as a high EC turnover. LWSS triggers the expression of the pro-inflammatory transcription factor NF-κB through JNK1-ATF2 activity, and induction of NF-κB-positive regulators (TLR, BMP, IKK2, ROS).[22] MCP-1 and VCAM-1 activation by OWSS is mediated by miR-21/PPARα/AP-1 signalling cascade.[71] OWSS also induces HDAC-3/5/7[72] and NLRP3-mediated inflammation.[73] Furthermore, disturbed flow promotes cell cycle progression via a sustained phosphorylation of Smad1/5 through integrin/BMP receptor association and the FAK/ERK cascade. Apoptosis is also increased through PKC-ζ, JNK-MAPK and p53 signalling.[22] Enhanced proliferation and apoptosis are typical signs of endothelium dysfunction.

Although many mechanosensors have been identified, the exact mechanism by which the signal transduction occurs in different flow conditions remains to be elucidated. Mechanotransduction has a pivotal role in vascular adaptation to a physiological range of flows. Disturbances in this process would clearly lead to similar consequences as pathological flow conditions. For example, defects in PC have been demonstrated to inhibit Ca^{2+} influx and NO synthesis in response to WSS. PC mutants are known to develop pathologies such as polycystic kidney disease and IAs. The potential role of PC in IA disease has been addressed in several studies.[62,63,74,75]

6.3 | Primary cilia: role in polycystic kidney disease and IAs

The primary cilium, in contrast to motile cilia, exists in a single structure at the cell surface and measures between 1 and 9 μm.[76] A so-called "9 + 0" arrangement defines the structure of its axoneme, where nine doublets of microtubules organize in a circumferential way, and the central part lacks the additional pair of microtubules, present in motile cilia (9 + 2). PC have gained importance in biomedical research as Pazour et al[77] revealed that the *Tg737* gene, whose mutation leads to renal polycystic disease in mice, encodes for a protein necessary for PC assembly. Further studies clearly confirmed that ADPKD is a ciliopathy. Indeed, ADPKD is a genetic disease caused by mutations in *PKD1* (85%) or *PKD2* (15%) genes leading to loss-of-function of polycystin-1 (PC1) and polycystin-2 (PC2), respectively.[78] PC1 and PC2 form a complex at the ciliary membrane and mediate Ca^{2+} influx into the cells. The PC1 C-terminal tail can bind and activate heterotrimeric G_i/G_o, but can also be cleaved and translocate into the nucleus and activate transcription factors, processes that are inhibited by interaction with PC2. PC2 functions as a transient cation channel and needs PC1 for its correct localization and activity.

Differences in cilium size, composition and morphology between cell types or organs testify the versatility of PC and their ability to recruit many different receptors to serve specific functions inherent to each cell type or organ. PC are involved in various cellular processes and the pathways regulated by PC comprise Wnt, Src, JNK, mTOR, JAK/STAT signalling among others.[78] In the vasculature, PC preferentially locate at arterial regions experiencing low flow and they have a critical role for EC structural integrity and function.[62,79-81] Thus, a non-functional PC would increase local injuries that can promote aneurysm formation and growth.[63] For instance, ADPKD patients show many extra-renal manifestations such as hepatic cyst, hypertension, left ventricular hypertrophy, pericardial effusions, cardiac valve abnormalities and IAs.[82] The development of IAs in ADPKD patients seems to results from PC impairment in the vasculature rather than from kidney failure. This is supported by the fact that 50% of ADPKD patients who receive a successful kidney transplantation still develop vascular complications[82] and that specific depletion of PC on ECs promotes IA development in mice.[63] Subsequently, it has been shown that PC in the endothelium are necessary for shear-induced Ca^{2+} influx and NO synthesis, events important for vascular contractility.[74,75] PC can also mediate SMC recruitment by ECs through the activation of Notch/foxc1b signalling during the vascular development.[61] Assuming that this process also occurs in adult blood vessels, it might be relevant for vascular repair and remodelling notably in IAs. In addition, PC absence in ECs has been associated with reduced level of hsp27 and reduced focal adhesion kinase phosphorylation leading to weaker stress fibers, impaired migration and reduced cellular barrier integrity.[83] The affected junctional proteins in this process still need to be unveiled. Indeed, loss of endothelium integrity is commonly observed in IAs and is a hallmark of wall instability as it promotes inflammatory cell infiltration.[84] In addition, PC absence has been associated with increases in inflammatory gene expression. Finally, mouse and human ECs lacking PC have been shown to be more sensitive to BMP-induced osteogenic differentiation, as a result of β-catenin and transcription factor Slug activation.[85] Interestingly, calcification has been reported in histological analyses of IAs as a marker of adverse outcome.[39]

7 | INTRACRANIAL ANEURYSM EXPERIMENTAL MODEL

Conducting research on PC and IA development relies on a representative and reproducible animal model. Even though in vitro cell models help to understand the mechanistic events, in vivo models provide integrative phenotypic clues onto the disease and they are essential for the development of diagnostic or therapeutic strategies. In Table 1, we have made a comprehensive overview of some of the animal models currently used to study the relationship between WSS and IAs. In brief, IAs rarely occur spontaneously in animals, therefore, induced IAs have been designed for experimental studies. IA induction relies on the principle that hemodynamic stress imposed on a fragile arterial wall will induce an aneurysmal out-pouching of the wall.[86] Hemodynamic stress is frequently increased by the induction of hypertension through renal artery ligation, angiotensin II infusion or high salt diet for example. Ligation of one common carotid artery would also increase the hemodynamic stress in the other common carotid artery (Table 1). The arterial wall is in general fragilized by chemical treatment such as elastase, an enzyme that breaks-down elastin and β-aminopropionitrile, which inhibits the cross-linking of collagen and elastin (Table 1). Various animal species can be used (mouse, rat, rabbit, dog, primate), and the choice relies on the experimental purpose. Although rodent models are easy to handle and relatively low-cost, the small size of their arteries is challenging for IA induction. Moreover, the small size of their cerebral arteries and IAs limits the possibility of radiological imaging or testing endovascular devices. The use of larger animals such as dogs and primates would overcome these hurdles, but they are more difficult to handle and thus restrict the number of animals that can be used. Rabbits

TABLE 1 Intracranial aneurysm experimental model

Study	Species	Genetic background	Methods for IA formation	Application
Hashimoto N, et al. Surg Neurol, 1978. **10**: 3	Rat	Wild-type	β-aminopropionitrile and elastase treatment + hypertension induced by deoxycorticosterone acetate or by ligation of the posterior branches of the renal arteries + high salt diet	–IA initiation
Hashimoto N, et al. J Neurosurg, 1987. **67**: 903	Monkey	Wild-type	Ligation of the posterior branch of left and right renal artery, and ligation of the left common carotid artery + diet containing NaCl and β-aminopropionitrile fumarate for >1 y	–IA incidence rate: 2/7 develop IA at 1 y. 5/7 with no IA detectable at the end of the study –Model for pharmacotherapy tests –Limitation: restricted number of animals, small size of IA (0.5-0.9 mm)
Coutard M, et al. Int J Exp Pathol, 1999. **80**: 357	Mouse	Blotchy mice (C57BL/6 J mo^{blo})	Ligation of the left common carotid artery + induced hypertension by ligation of renal arteries during 6-12 mo	–17%-38% incidence with small and large size IA –Testing of endovascular devices –Model for pharmacotherapy tests –Limitation: high percentage of death due to surgical procedure (30%-40%)
Altes T.A, et al. AJR Am J Roentgenol, 2000. **174**: 349 Wang S, et al. J Neurointerv Surg, 2018. **10**: 411	Rabbit	Wild-type	Elastase treatment + ligation of the common carotid artery for 2-24 wk	–89% IA incidence rate –Study of unorganized thrombus –Testing of endovascular devices –Limitation: big size aneurysm but risk of elastase intoxication
Morimoto M, et al. Stroke, 2002. **33**: 1911	Mouse	Wild-type	Ligations of the left common carotid artery and posterior branches of bilateral renal arteries + high salt diet during 4 wk	–77% IA incidence rate –Limitation: early aneurysm changes observed only in microscopic studies
Frosen J, et al. Neurosurgery, 2006. **58**: 936	Mouse and Rat	Wild-type	Microsurgical grafts on the lateral wall of the abdominal aorta during 3 d to 3 mo	–100% aneurysm induction –Testing of endovascular device –Model for IA growth
Moriwaki T, et al. Stroke, 2006. **37**: 900	Mouse	Wild-type	Ligation of the left common carotid artery and the posterior branch of the left and right renal artery + high salt diet containing β-aminopropionitrile during 3-5 mo	–23%-31% IA incidence rate –30% early aneurysm changes –30% advanced stage aneurysm
Abruzzo T, et al. Curr Neurovasc Res, 2007. **4**: 161	Mouse	$eNOS^{-/-}$	Ligation of the left common carotid artery for 13 mo	–30% IA incidence rate
Meng H, et al. Stroke, 2007. **38**: 1924	Dog	Wild-type	Surgically created bifurcation between left and right common carotid arteries + high salt diet + renal artery ligation during 2 wk to 2 mo	–100% IA incidence rate of early aneurysm change –Limitation: early aneurysm changes observed only in microscopic studies
Nuki Y, et al. Hypertension, 2009. **54**: 1337	Mouse	Wild-type	Angiotensin II and elastase treatment for 2 wk	–77% IA incidence rate –Limitation: small size IA, early aneurysm changes

(Continues)

TABLE 1 (Continued)

Study	Species	Genetic background	Methods for IA formation	Application
Metaxa E, et al. Stroke, 2010. **41**: 1774 Gao L, et al. Stroke, 2008. **39**: 2085	Rabbit	Wild-type	Bilateral common carotid arteries ligation for 5 d to 12 wk	–100% IA incidence rate of early aneurysm changes
Makino H, et al. Stroke, 2012. **43**: 2450	Mouse	Wild-type	Deoxycorticosterone acetate-salt hypertension + elastase treatment for 7-28 d	–63% incidence rate within 7 d –40% rupture rate after 28 d –Model for pharmacotherapy tests
Hosaka K, et al. J Neurointerv Surg, 2014. **6**: 474	Mouse	Wild-type	Ligation of the right renal artery and the left common carotid artery + angiotensin II and elastase treatment + hypertensive diet containing β-aminopropionitrile during 3 wk	–90%-100% IA incidence rate –20%-60% IA rupture rate
Liu M, et al. Shock, 2018. **49**: 604	Mouse	Endothelial cell specific knockout of *PKD1*, *PKD2* or *IFT88*	Angiotensin II and elastase treatment during 20 d, 4 wk after gene excision	–60%-100% incidence –60%-100% rupture rate –Model for pharmacotherapy tests

IA, intracranial aneurysm; d, day; wk, week; mo, months.

seem to be a good compromise, and the diameter of their extracranial carotid arteries is similar to humans.[87] Another frequently used technique for experimental IAs is the surgically created model, where an arterial or venous pouch from a donor animal is end-to-side or side-to-side grafted to an arterial wall of a recipient animal.[88] The main advantage of this technique is that it gives more freedom onto the choice of the IA size, orientation and localization. It is therefore very suitable for testing of endovascular devices. The recent development of CRISPR/Cas9-induced genetic modifications in multiple animal species will certainly be helpful to further unravel the pathophysiology of IA growth and rupture in relation to hemodynamic forces in experimental IA models.

8 | CONCLUSION

There is so far no specific treatment to prevent IA growth or rupture. When clinicians estimate a high risk of rupture, surgical clipping or endovascular coiling remain the only options. However, an accurate assessment of the risk of rupture remains challenging and most likely leads to an overtreatment of IAs. Accumulating evidences obtained from studies combining IA histology and CFD stress out the critical role of WSS and mechanotransduction in IA pathology. The most direct proof for such critical relation perhaps comes from the fact that genetic mutations leading to PC dysfunction predispose ADPKD patients to more IA formation with a severe phenotype. In depth knowledge of how vascular cells respond to WSS, including analyses of the acute repair and the chronic degenerative processes, would help us to understand the molecular and cellular events leading to IA growth and rupture. Such information would be valuable for the development of new biomarkers to accurately characterize the state of the disease, but also for the development of new drugs to prevent IA progression.

ACKNOWLEDGEMENTS

This work was supported by the grants from the Swiss SystemsX.ch initiative, evaluated by the Swiss National Science Foundation (to PB and BRK) and the Swiss Heart Foundation (to BRK and PB). We thank Marie-Luce Bochaton-Piallat, Esther Sutter and Vincent Braunersreuther (Department of Pathology and Immunology, University of Geneva) for antibodies or technical help with histology.

CONFLICT OF INTEREST

The authors have no conflicts of interest to declare.

ORCID

Brenda R. Kwak http://orcid.org/0000-0003-0015-0044

REFERENCES

1. Brisman JL, Song JK, Newell DW. Cerebral aneurysms. *N Engl J Med*. 2006;355(9):928-939.
2. Vlak MH, Rinkel GJ, Greebe P, van der Bom JG, Algra A. Trigger factors for rupture of intracranial aneurysms in relation to patient and aneurysm characteristics. *J Neurol*. 2012;259(7):1298-1302.
3. Etminan N, Rinkel GJ. Unruptured intracranial aneurysms: development, rupture and preventive management. *Nat Rev Neurol*. 2016;12(12):699-713.
4. Kotowski M, Naggara O, Darsaut TE, et al. Safety and occlusion rates of surgical treatment of unruptured intracranial aneurysms: a systematic review and meta-analysis of the literature from 1990 to 2011. *J Neurol Neurosurg Psychiatry*. 2013;84(1):42-48.
5. Naggara ON, White PM, Guilbert F, Roy D, Weill A, Raymond J. Endovascular treatment of intracranial unruptured aneurysms: systematic review and meta-analysis of the literature on safety and efficacy. *Radiology*. 2010;256(3):887-897.
6. Greving JP, Wermer MJ, Brown Jr RD, et al. Development of the PHASES score for prediction of risk of rupture of intracranial aneurysms: a pooled analysis of six prospective cohort studies. *Lancet Neurol*. 2014;13(1):59-66.
7. Etminan N, Brown Jr RD, Beseoglu K, et al. The unruptured intracranial aneurysm treatment score: a multidisciplinary consensus. *Neurology*. 2015;85(10):881-889.
8. Backes D, Rinkel GJE, Greving JP, et al. ELAPSS score for prediction of risk of growth of unruptured intracranial aneurysms. *Neurology*. 2017;88(17):1600-1606.
9. Bijlenga P, Gondar R, Schilling S, et al. PHASES score for the management of intracranial aneurysm: a cross-sectional population-based retrospective study. *Stroke*. 2017;48(8):2105-2112.
10. Varble N, Tutino VM, Yu J, et al. Shared and distinct rupture discriminants of small and large intracranial aneurysms. *Stroke*. 2018;49:856-864.
11. Inoue T, Shimizu H, Fujimura M, Saito A, Tominaga T. Annual rupture risk of growing unruptured cerebral aneurysms detected by magnetic resonance angiography. *J Neurosurg*. 2012;117(1):20-25.
12. Villablanca JP, Duckwiler GR, Jahan R, et al. Natural history of asymptomatic unruptured cerebral aneurysms evaluated at CT angiography: growth and rupture incidence and correlation with epidemiologic risk factors. *Radiology*. 2013;269(1):258-265.
13. Boussel L, Rayz V, McCulloch C, et al. Aneurysm growth occurs at region of low wall shear stress: patient-specific correlation of hemodynamics and growth in a longitudinal study. *Stroke*. 2008;39(11):2997-3002.
14. Castro MA, Putman CM, Sheridan MJ, Cebral JR. Hemodynamic patterns of anterior communicating artery aneurysms: a possible association with rupture. *AJNR Am J Neuroradiol*. 2009;30(2):297-302.
15. Cebral JR, Mut F, Weir J, Putman C. Quantitative characterization of the hemodynamic environment in ruptured and unruptured brain aneurysms. *AJNR Am J Neuroradiol*. 2011;32(1):145-151.
16. Fukazawa K, Ishida F, Umeda Y, et al. Using computational fluid dynamics analysis to characterize local hemodynamic features of middle cerebral artery aneurysm rupture points. *World Neurosurg*. 2015;83(1):80-86.
17. Miura Y, Ishida F, Umeda Y, et al. Low wall shear stress is independently associated with the rupture status of middle cerebral artery aneurysms. *Stroke*. 2013;44(2):519-521.
18. Xiang J, Natarajan SK, Tremmel M, et al. Hemodynamic-morphologic discriminants for intracranial aneurysm rupture. *Stroke*. 2011;42(1):144-152.
19. Zhou G, Zhu Y, Yin Y, Su M, Li M. Association of wall shear stress with intracranial aneurysm rupture: systematic review and meta-analysis. *Sci Rep*. 2017;7(1):5331.
20. Machi P, Ouared R, Brina O, et al. Hemodynamics of focal versus global growth of small cerebral aneurysms. *Clin Neuroradiol*. 2017;27:1-9.
21. Lv N, Wang C, Karmonik C, et al. Morphological and hemodynamic discriminators for rupture status in posterior communicating artery aneurysms. *PLoS One*. 2016;11(2):e0149906.
22. Kwak BR, Back M, Bochaton-Piallat ML, et al. Biomechanical factors in atherosclerosis: mechanisms and clinical implications. *Eur Heart J*. 2014;35(43):3013-3020, 3020a-3020d.
23. Zhao X, Zhao M, Amin-Hanjani S, Du X, Ruland S, Charbel FT. Wall shear stress in major cerebral arteries as a function of age and gender–a study of 301 healthy volunteers. *J Neuroimaging*. 2015;25(3):403-407.
24. Davies PF. Hemodynamic shear stress and the endothelium in cardiovascular pathophysiology. *Nat Clin Pract Cardiovasc Med*. 2009;6(1):16-26.
25. Ku DN. Blood flow in arteries. *Annu Rev Fluid Mech*. 1997;29(1):399-434.
26. Alnaes MS, Isaksen J, Mardal KA, Romner B, Morgan MK, Ingebrigtsen T. Computation of hemodynamics in the circle of Willis. *Stroke*. 2007;38(9):2500-2505.
27. Meng H, Wang Z, Hoi Y, et al. Complex hemodynamics at the apex of an arterial bifurcation induces vascular remodeling resembling cerebral aneurysm initiation. *Stroke*. 2007;38(6):1924-1931.
28. Anwar MA, Shalhoub J, Lim CS, Gohel MS, Davies AH. The effect of pressure-induced mechanical stretch on vascular wall differential gene expression. *J Vasc Res*. 2012;49(6):463-478.
29. Cebral JR, Putman CM, Alley MT, Hope T, Bammer R, Calamante F. Hemodynamics in normal cerebral arteries: qualitative comparison of 4D phase-contrast magnetic resonance and image-based computational fluid dynamics. *J Eng Math*. 2009;64(4):367-378.
30. Grinberg L, Anor T, Cheever E, Madsen JR, Karniadakis GE. Simulation of the human intracranial arterial tree. *Philos Trans A Math Phys Eng Sci*. 1896;2009(367):2371-2386.
31. Bor AS, Velthuis BK, Majoie CB, Rinkel GJ. Configuration of intracranial arteries and development of aneurysms: a follow-up study. *Neurology*. 2008;70(9):700-705.
32. Lazzaro MA, Ouyang B, Chen M. The role of circle of Willis anomalies in cerebral aneurysm rupture. *J Neurointerv Surg*. 2012;4(1):22-26.
33. Liu Z, Cai Y, Chen G-Z, Lu G-M, Li Z-Y. Anatomical variations in circle of Willis and intracranial aneurysm formation. *Mol Cell Biomech*. 2017;14(1):19-31.
34. Nam SW, Choi S, Cheong Y, Kim YH, Park HK. Evaluation of aneurysm-associated wall shear stress related to morphological

variations of circle of Willis using a microfluidic device. *J Biomech*. 2015;48(2):348-353.
35. Kapoor K, Singh B, Dewan LI. Variations in the configuration of the circle of Willis. *Anat Sci Int*. 2008;83(2):96-106.
36. Etminan N, Buchholz BA, Dreier R, et al. Cerebral aneurysms: formation, progression, and developmental chronology. *Transl Stroke Res*. 2014;5(2):167-173.
37. Aoki T, Kataoka H, Shimamura M, et al. NF-kappaB is a key mediator of cerebral aneurysm formation. *Circulation*. 2007;116 (24):2830-2840.
38. Stehbens WE. Histopathology of cerebral aneurysms. *Arch Neurol*. 1963;8:272-285.
39. Frosen J, Piippo A, Paetau A, et al. Remodeling of saccular cerebral artery aneurysm wall is associated with rupture: histological analysis of 24 unruptured and 42 ruptured cases. *Stroke*. 2004;35 (10):2287-2293.
40. Frosen J, Tulamo R, Heikura T, et al. Lipid accumulation, lipid oxidation, and low plasma levels of acquired antibodies against oxidized lipids associate with degeneration and rupture of the intracranial aneurysm wall. *Acta Neuropathol Commun*. 2013;1:71.
41. Kataoka K, Taneda M, Asai T, Kinoshita A, Ito M, Kuroda R. Structural fragility and inflammatory response of ruptured cerebral aneurysms. A comparative study between ruptured and unruptured cerebral aneurysms. *Stroke*. 1999;30(7):1396-1401.
42. Korkmaz E, Kleinloog R, Verweij BH, et al. Comparative ultrastructural and stereological analyses of unruptured and ruptured saccular intracranial aneurysms. *J Neuropathol Exp Neurol*. 2017;76(10):908-916.
43. Tulamo R, Frosen J, Junnikkala S, et al. Complement activation associates with saccular cerebral artery aneurysm wall degeneration and rupture. *Neurosurgery*. 2006;59(5):1069-1076; discussion 1076-1067.
44. Morel S, Diagbouga MR, Dupuy N, et al. Correlating clinical risk factors and histological features in ruptured and unruptured human intracranial aneurysms: the Swiss AneuX Study. *J Neuropathol Exp Neurol*. 2018;77:555-566.
45. Frosen J, Tulamo R, Paetau A, et al. Saccular intracranial aneurysm: pathology and mechanisms. *Acta Neuropathol*. 2012;123 (6):773-786.
46. Davies PF, Civelek M, Fang Y, Fleming I. The atherosusceptible endothelium: endothelial phenotypes in complex haemodynamic shear stress regions in vivo. *Cardiovasc Res*. 2013;99(2):315-327.
47. Chiu JJ, Chien S. Effects of disturbed flow on vascular endothelium: pathophysiological basis and clinical perspectives. *Physiol Rev*. 2011;91(1):327-387.
48. Aoki T, Yamamoto K, Fukuda M, Shimogonya Y, Fukuda S, Narumiya S. Sustained expression of MCP-1 by low wall shear stress loading concomitant with turbulent flow on endothelial cells of intracranial aneurysm. *Acta Neuropathol Commun*. 2016;4(1):48.
49. Rempe RG, Hartz AM, Bauer B. Matrix metalloproteinases in the brain and blood-brain barrier: versatile breakers and makers. *J Cereb Blood Flow Metab*. 2016;36(9):1481-1507.
50. Wang Z, Kolega J, Hoi Y, et al. Molecular alterations associated with aneurysmal remodeling are localized in the high hemodynamic stress region of a created carotid bifurcation. *Neurosurgery*. 2009;65(1):169-177; discussion 177-168.
51. Dolan JM, Meng H, Singh S, Paluch R, Kolega J. High fluid shear stress and spatial shear stress gradients affect endothelial proliferation, survival, and alignment. *Ann Biomed Eng*. 2011;39 (6):1620-1631.
52. Metaxa E, Tremmel M, Natarajan SK, et al. Characterization of critical hemodynamics contributing to aneurysmal remodeling at the basilar terminus in a rabbit model. *Stroke*. 2010;41(8):1774-1782.
53. Alfano JM, Kolega J, Natarajan SK, et al. Intracranial aneurysms occur more frequently at bifurcation sites that typically experience higher hemodynamic stresses. *Neurosurgery*. 2013;73 (3):497-505.
54. Can A, Castro VM, Ozdemir YH, et al. Association of intracranial aneurysm rupture with smoking duration, intensity, and cessation. *Neurology*. 2017;89(13):1408-1415.
55. Meng H, Tutino VM, Xiang J, Siddiqui A. High WSS or low WSS? Complex interactions of hemodynamics with intracranial aneurysm initiation, growth, and rupture: toward a unifying hypothesis. *AJNR Am J Neuroradiol*. 2014;35(7):1254-1262.
56. Castro M, Putman C, Radaelli A, Frangi A, Cebral J. Hemodynamics and rupture of terminal cerebral aneurysms. *Acad Radiol*. 2009;16(10):1201-1207.
57. Mut F, Lohner R, Chien A, et al. Computational hemodynamics framework for the analysis of cerebral aneurysms. *Int J Numer Method Biomed Eng*. 2011;27(6):822-839.
58. Cebral J, Ollikainen E, Chung BJ, et al. Flow conditions in the intracranial aneurysm lumen are associated with inflammation and degenerative changes of the aneurysm wall. *AJNR Am J Neuroradiol*. 2017;38(1):119-126.
59. White CR, Frangos JA. The shear stress of it all: the cell membrane and mechanochemical transduction. *Philos Trans R Soc Lond B Biol Sci*. 2007;362(1484):1459-1467.
60. Givens C, Tzima E. Endothelial mechanosignaling: does one sensor fit all? *Antioxid Redox Signal*. 2016;25(7):373-388.
61. Chen X, Gays D, Milia C, Santoro MM. Cilia control vascular mural cell recruitment in vertebrates. *Cell Rep*. 2017;18(4):1033-1047.
62. Nauli SM, Kawanabe Y, Kaminski JJ, Pearce WJ, Ingber DE, Zhou J. Endothelial cilia are fluid shear sensors that regulate calcium signaling and nitric oxide production through polycystin-1. *Circulation*. 2008;117(9):1161-1171.
63. Liu M, Zhao J, Zhou Q, Peng Y, Zhou Y, Jiang Y. Primary cilia deficiency induces intracranial aneurysm. *Shock*. 2018;49(5):604-611.
64. Wang N, Tytell JD, Ingber DE. Mechanotransduction at a distance: mechanically coupling the extracellular matrix with the nucleus. *Nat Rev Mol Cell Biol*. 2009;10(1):75-82.
65. Dimmeler S, Fleming I, Fisslthaler B, Hermann C, Busse R, Zeiher AM. Activation of nitric oxide synthase in endothelial cells by Akt-dependent phosphorylation. *Nature*. 1999;399(6736):601-605.
66. Fisslthaler B, Loot AE, Mohamed A, Busse R, Fleming I. Inhibition of endothelial nitric oxide synthase activity by proline-rich tyrosine kinase 2 in response to fluid shear stress and insulin. *Circ Res*. 2008;102(12):1520-1528.
67. Young A, Wu W, Sun W, et al. Flow activation of AMP-activated protein kinase in vascular endothelium leads to Kruppel-like factor 2 expression. *Arterioscler Thromb Vasc Biol*. 2009;29 (11):1902-1908.
68. Wu W, Xiao H, Laguna-Fernandez A, et al. Flow-dependent regulation of Kruppel-like factor 2 is mediated by microRNA-92a. *Circulation*. 2011;124(5):633-641.

69. Ni CW, Wang DL, Lien SC, Cheng JJ, Chao YJ, Hsieh HJ. Activation of PKC-epsilon and ERK1/2 participates in shear-induced endothelial MCP-1 expression that is repressed by nitric oxide. *J Cell Physiol*. 2003;195(3):428-434.
70. Gongol B, Marin T, Peng IC, et al. AMPKalpha2 exerts its anti-inflammatory effects through PARP-1 and Bcl-6. *Proc Natl Acad Sci U S A*. 2013;110(8):3161-3166.
71. Zhou J, Wang KC, Wu W, et al. MicroRNA-21 targets peroxisome proliferators-activated receptor-alpha in an autoregulatory loop to modulate flow-induced endothelial inflammation. *Proc Natl Acad Sci U S A*. 2011;108(25):10355-10360.
72. Lee DY, Lee CI, Lin TE, et al. Role of histone deacetylases in transcription factor regulation and cell cycle modulation in endothelial cells in response to disturbed flow. *Proc Natl Acad Sci U S A*. 2012;109(6):1967-1972.
73. Xiao H, Lu M, Lin TY, et al. Sterol regulatory element binding protein 2 activation of NLRP3 inflammasome in endothelium mediates hemodynamic-induced atherosclerosis susceptibility. *Circulation*. 2013;128(6):632-642.
74. AbouAlaiwi WA, Takahashi M, Mell BR, et al. Ciliary polycystin-2 is a mechanosensitive calcium channel involved in nitric oxide signaling cascades. *Circ Res*. 2009;104(7):860-869.
75. Nauli SM, Alenghat FJ, Luo Y, et al. Polycystins 1 and 2 mediate mechanosensation in the primary cilium of kidney cells. *Nat Genet*. 2003;33(2):129-137.
76. Dummer A, Poelma C, DeRuiter MC, Goumans MJ, Hierck BP. Measuring the primary cilium length: improved method for unbiased high-throughput analysis. *Cilia*. 2016;5:7.
77. Pazour GJ, Dickert BL, Vucica Y, et al. Chlamydomonas IFT88 and its mouse homologue, polycystic kidney disease gene tg737, are required for assembly of cilia and flagella. *J Cell Biol*. 2000;151(3):709-718.
78. Lemos FO, Ehrlich BE. Polycystin and calcium signaling in cell death and survival. *Cell Calcium*. 2018;69:37-45.
79. Iomini C, Tejada K, Mo W, Vaananen H, Piperno G. Primary cilia of human endothelial cells disassemble under laminar shear stress. *J Cell Biol*. 2004;164(6):811-817.
80. Van der Heiden K, Groenendijk BC, Hierck BP, et al. Monocilia on chicken embryonic endocardium in low shear stress areas. *Dev Dyn*. 2006;235(1):19-28.
81. Aboualaiwi WA, Muntean BS, Ratnam S, et al. Survivin-induced abnormal ploidy contributes to cystic kidney and aneurysm formation. *Circulation*. 2014;129(6):660-672.
82. Luciano RL, Dahl NK. Extra-renal manifestations of autosomal dominant polycystic kidney disease (ADPKD): considerations for routine screening and management. *Nephrol Dial Transplant*. 2014;29(2):247-254.
83. Jones TJ, Adapala RK, Geldenhuys WJ, et al. Primary cilia regulates the directional migration and barrier integrity of endothelial cells through the modulation of hsp27 dependent actin cytoskeletal organization. *J Cell Physiol*. 2012;227(1):70-76.
84. Yamamoto R, Aoki T, Koseki H, et al. A sphingosine-1-phosphate receptor type 1 agonist, ASP4058, suppresses intracranial aneurysm through promoting endothelial integrity and blocking macrophage transmigration. *Br J Pharmacol*. 2017;174(13):2085-2101.
85. Sanchez-Duffhues G, de Vinuesa AG, Lindeman JH, et al. SLUG is expressed in endothelial cells lacking primary cilia to promote cellular calcification. *Arterioscler Thromb Vasc Biol*. 2015;35(3):616-627.
86. Hashimoto N, Handa H, Hazama F. Experimentally induced cerebral aneurysms in rats. *Surg Neurol*. 1978;10(1):3-8.
87. Altes TA, Cloft HJ, Short JG, et al. 1999 ARRS Executive Council Award. Creation of saccular aneurysms in the rabbit: a model suitable for testing endovascular devices. American Roentgen Ray Society. *AJR Am J Roentgenol*. 2000;174(2):349-354.
88. Frosen J, Marjamaa J, Myllarniemi M, et al. Contribution of mural and bone marrow-derived neointimal cells to thrombus organization and wall remodeling in a microsurgical murine saccular aneurysm model. *Neurosurgery*. 2006;58(5):936-944; discussion 936-944.

How to cite this article: Diagbouga MR, Morel S, Bijlenga P, Kwak BR. Role of hemodynamics in initiation/growth of intracranial aneurysms. *Eur J Clin Invest*. 2018;48:e12992. https://doi.org/10.1111/eci.12992